IOP Publishing Journal of Neural Engineering
J. Neural Eng. 13 (2016) 036017 (8pp) doi:10.1088/1741-2560/13/3/036017

Asynchronous decoding of finger movements from ECoG signals using long-range dependencies conditional random fields

Jaime F Delgado Saa[1,4], Adriana de Pesters[2] and Mujdat Cetin[3]

[1] Universidad del Norte, Biomedical Signal Processing and Artificial Intelligence Laboratory, Barranquilla, Colombia
[2] National Center for Adaptive Neurotechnologies, Schalk Lab, Albany, NY, USA
[3] Sabanci University, Signal Processing and Information Systems Laboratory, Istanbul, Turkey

E-mail: jadelgado@uninorte.edu.co, jfdelgad@gmail.com, adepesters@gmail.com and mceting@sabanciuniv.edu

Received 15 November 2015, revised 25 March 2016
Accepted for publication 14 April 2016
Published 3 May 2016

Abstract

Objective. In this work we propose the use of conditional random fields with long-range dependencies for the classification of finger movements from electrocorticographic recordings. *Approach*. The proposed method uses long-range dependencies taking into consideration time-lags between the brain activity and the execution of the motor task. In addition, the proposed method models the dynamics of the task executed by the subject and uses information about these dynamics as prior information during the classification stage. *Main results*. The results show that incorporating temporal information about the executed task as well as incorporating long-range dependencies between the brain signals and the labels effectively increases the system's classification performance compared to methods in the state of art. *Significance*. The method proposed in this work makes use of probabilistic graphical models to incorporate temporal information in the classification of finger movements from electrocorticographic recordings. The proposed method highlights the importance of including prior information about the task that the subjects execute. As the results show, the combination of these two features effectively produce a significant improvement of the system's classification performance.

Keywords: Brain-computer interfaces, ECoG, synchronous classification, temporal dynamics, probabilistic graphical models

(Some figures may appear in colour only in the online journal)

1. Introduction

A brain-computer interface (BCI) provides an alternative communication path with the environment for people suffering from diseases that produce a loss of motor control. The lack of ability to communicate with the environment considerably affects the quality of life of such individuals, and restoring this ability is the main motivation for the development of BCIs. Although most BCIs make use of electroencephalography (EEG) recordings, a considerable amount of work using electrocorticographic (ECoG) recordings has been done in the last decade and BCIs based on ECoG have been proposed previously [1–7].

BCIs based on sensorimotor rhythms rely on the fact that the execution of an imaginary motor task involves the same cortical areas required to execute an actual movement [8]. The poor spatial resolution of EEG limits the tasks to be executed by the subject to imaginary movements involving large

[4] Author to whom any correspondence should be addressed.

cortical areas, as is the case for movements of the arms, legs, feet, etc. In contrast, the high spatial resolution of ECoG allows researchers to predict motor activity related to more specific body parts. For example, individual finger movements can be predicted or decoded using ECoG recordings [9–13]. One aspect of ECoG that makes this possible is that the spectrum of frequencies that can be recorded with ECoG goes far beyond that of EEG. In practice, a limit of 40Hz is usually assumed for EEG recordings, whereas in ECoG recordings, frequency components up to 200 Hz can be observed. In particular, the power of the signal components with frequencies in the range of 70 to 200 Hz reflect the neuronal activity of areas in the cortex that are related to the execution of specific tasks [14].

Several previous works considered the problem of finger movement decoding in synchronous and asynchronous scenarios. In a synchronous scenario the subjects are requested to perform a particular task at a particular instant, therefore the beginning and the end of the performed task are known *a priori* in the training set as well as for the testing set. In [11] a set of features based on the amplitude of the ECoG signals in different frequency bands are used for classification of finger movement in a synchronous scenario. The authors compare Hidden Markov Models (HMM) and Support Vector Machines (SVM) showing that the results obtained with these classifiers are comparable. Interestingly, it was shown in [11] that the results obtained with HMM can be improved by restricting the structure of the model so as not to allow transitions to previously visited states. More recently, also in a synchronous scenario, the authors in [12] have shown that it is possible to classify finger movements above the chance level using EEG recordings. In this approach the features are obtained using spectral decomposition of the EEG signal and principal component analysis. Subsequently, classification is done using SVM. The same technique was applied to ECoG data in [12] showing good performance with accuracy above 90%. In [10], a different approach is taken by including prior information about the movement of the fingers. This prior information corresponds to the patterns of finger flexion and finger extension executed by the subject. The method proposed in [10] makes use of a Bayesian decoding method to incorporate the constrains about flexion/extension of the fingers in the graphical structure of a probabilist model. Although this approach does not aim to improve the classification rate related to which finger moves, it is suggested by the authors that it provides a better estimation of the flexion and extension of a particular finger.

In an asynchronous scenario, the authors in [9] show that it is possible to decode the flexion and extension of individual fingers with reasonable precision. For this, brain signals from the area contralateral to the hand executing the movement were recorded. A linear combination of the brain signals was used to predict the time course signal that describes the flexion and extension of the fingers. Similar results were obtained in [13] where a switching linear model was employed. The authors in [13] proposed an inference approach composed of two main blocks. The first block is composed of a linear model that infers which finger is moving. The linear model proposed is learned using simultaneous sparse approximation (SSA) which provides a sparse solution aiming to avoid over-fitting. The output of the first block determines which finger is moving and it is used by the second block to select a model (one for each finger plus one model for rest periods) that describes the dynamics of the movements. In this approach, correct classification of the moving finger (first block output) is critical for the inference of the flexion and extension of the fingers (second block output). With a similar perspective, the authors in [15] proposed a method based on principal component analysis (PCA) and machine learning techniques such as linear discriminant analysis and support vector machines for the classification of finger movements.

In the last decade, techniques based on probabilistic graphical models have been proposed for BCI [10, 16–21]. These techniques have the advantage of being probabilistic approaches that provide an integrative framework for BCI systems. They have the ability to incorporate information about the temporal dynamics of the task that the subject is executing [18] and also the temporal dynamics of the brain signals [17, 21].

In this work we propose the use of a probabilistic graphical model approach based on conditional random fields (CRF) for asynchronous classification of finger's movements from ECoG signals. The proposed method incorporates information about the temporal dynamics of the task as prior information. The results show that incorporating temporal information on the modeling of the ECoG signals significantly improves the ability of the a BCI system to predict finger movements, compared to existing methods for asynchronous classification.

2. Signal analysis

2.1. Dataset description

We used an ECoG dataset publicly available from the BCI competition IV [22]. ECoG signals from three subjects were recorded over the course of 10 minutes. The subjects sat in front of a screen and were requested to move their fingers according to a stimulus presented on the screen indicating the name of the finger to move. The cue was displayed for two seconds and was followed by two seconds of rest. During the rest periods the screen was blank. Additionally, the subjects wore a data-glove that was used to record the actual movement of the fingers. Signals from the data-glove are used as ground truth. ECoG signals were recorded using a grid of electrodes (the number of electrodes was different for each subject) ranging from 48 to 64 electrodes. The subjects were required to execute the movements with the hand contralateral to the placement of the grid of electrodes. The sampling frequency was set to 1000Hz for the ECoG recordings and 25 Hz for the data-glove. Given that the data-glove signals are available, these can be used to determine the beginning and end of the finger's movement which makes it possible to treat this problem as a synchronous problem. However, we

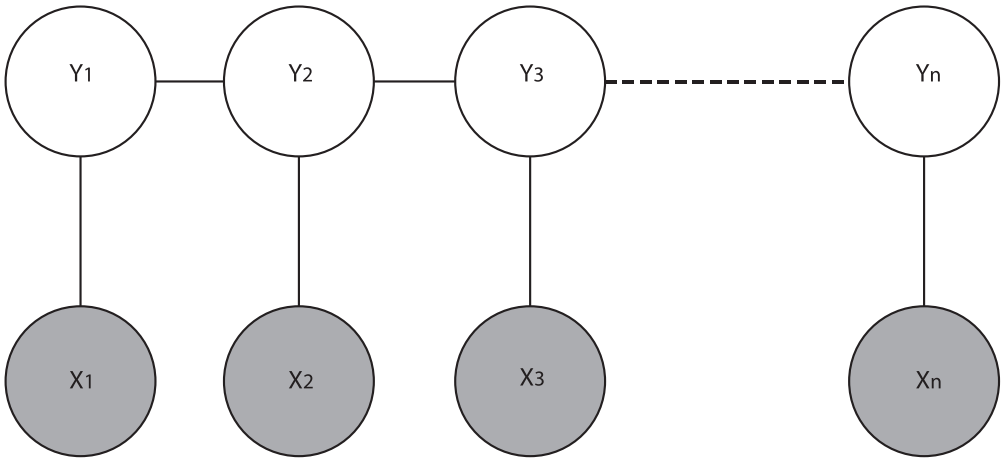

Figure 1. The CRF Model. The circles represent variables and the lines represent direct dependencies. The shaded circles represent observed variables. The brain signal features extracted from the ECoG signals are represented by the variable $\mathbf{x} = \{x_1, \ldots, x_n\}$, and the labels that indicate which finger is in motion are represented by the variable $\mathbf{y} = \{y_1, \ldots, y_n\}$.

developed an asynchronous approach as this more closely resembles the actual mode of operation of practical BCIs.

2.2. Frequency selection and feature extraction

Frequency components of the brain signals in the range of 70—170 Hz (high gamma) were extracted using a band-pass Butterworth IIR filter of order eight. The limits of the frequency bands were selected to avoid the first and third harmonic of the 60 Hz line noise. Based on previous work [23] it is assumed that the power of the brain signals in high gamma is correlated with neuronal firing rate and neural synchrony in regions related to the execution of a specific task. We calculated the envelope of band-passed brain signals using the absolute value of the analytic signal, which is calculated with the help of the Hilbert transform. The envelope obtained was then low-pass filtered to allow frequencies up to 6 Hz. The value of 6 Hz was selected because it is the maximum frequency at which the subject moves the finger, and the envelope of the ECoG signals in the selected frequency band is assumed to reflect the dynamics of the task [9, 24]. In particular for the task executed by the subjects in this work, the power in high-gamma is assumed to be correlated with movement of the fingers, and therefore muscle activity. The filtered envelope was downsampled taking samples every 50 ms.

3. CRFs for classification of finger movements

The classification task corresponds to labeling the periods of time during which one specific finger is moving. For this, we build a conditional random field (CRF) for modeling the activity of all fingers. This scenario describes a six-class classification problem that includes the movement of five fingers and rest periods.

Referring to figure 1, the brain signal features (envelope of high gamma in each electrode) are represented by $\mathbf{x} = \{x_1, \ldots, x_n\}$, where n represents the time points and $x_i \in R^d$, where d is the number of electrodes. The labels, the ground truths of which are obtained from the data-glove signals, are represented by $\mathbf{y} = \{y_1, \ldots, y_n\}$, with $y \in [1, 6]$, with 1, 2, 3, 4, 5, 6 representing resting, movement of thumb, index, middle, ring and pinky fingers, respectively.

The conditional probability of the labels given the observed brain signal features is modeled as:

$$p(\mathbf{y}|\mathbf{x}, \Theta) = \frac{1}{Z} \prod_{i=1}^{n} \Psi_i(y_i, x_i) \prod_{i=2}^{n} \Phi_i(y_i, y_{i-1}) \tag{1}$$

where Z is a normalization factor, $\Psi_i(y_i, x_i)$ is a node potential function and $\Phi_i(y_i, y_{i-1})$ is an edge potential function. The node potential functions are defined according to:

$$\Psi_i(y_i, x_i) = e^{\sum_{j=1}^{d} \theta_{vj}^T f_{vj}(x_{i,j}, y_i)} \tag{2}$$

where $f_{vj}(x_{i,j}, y_i) = 1_{y_i} x_{i,j}$, where 1_{y_i} is a column vector with a non-zero entry in the y_i position and with length equal to six (the number of classes); $x_{i,j}$ is a real number. The parameter θ_{vj} is a set of weights, one for each class, which has the same size of 1_{y_i}. The expression $\sum_{j=1}^{d} \theta_{vj}^T f_{vj}(x_{i,j}, y_i)$ is a measure of the compatibility between the brain signals x_i and the movement of the finger represented by the label y_i.

In the particular case of the application addressed in the present work, the movement of the fingers lags brain signals activity in the selected frequency band by 50 to 100 ms [9]. In order to include this information in the model, we modify the standard CRF-chain shown in figure 3 to allow the inclusion of long range dependencies as presented in figure 2. These long range dependencies allow samples in past time instants to be included in the prediction of the label at the current time point. In order to include this characteristic in the model, we modify the potential function in equation (2) as follows:

$$\Psi_i(y_i, x_{(i-k:i)}) = e^{\sum_{j=1}^{d} \sum_{l=0}^{k-1} \theta_{v(k,j)}^T f_{vj}(x_{(i-k,j)}, y_i)} \tag{3}$$

where $x_{i-k:i} = \{x_{i-k}, x_{i-k+1}, \ldots, x_i\}$. The index k defines the number of samples previous to the current time point i that are used to predict the label y_i. The function f_{vj} is the same described above and the parameter $\theta_{vk,j}$ is an augmented set of

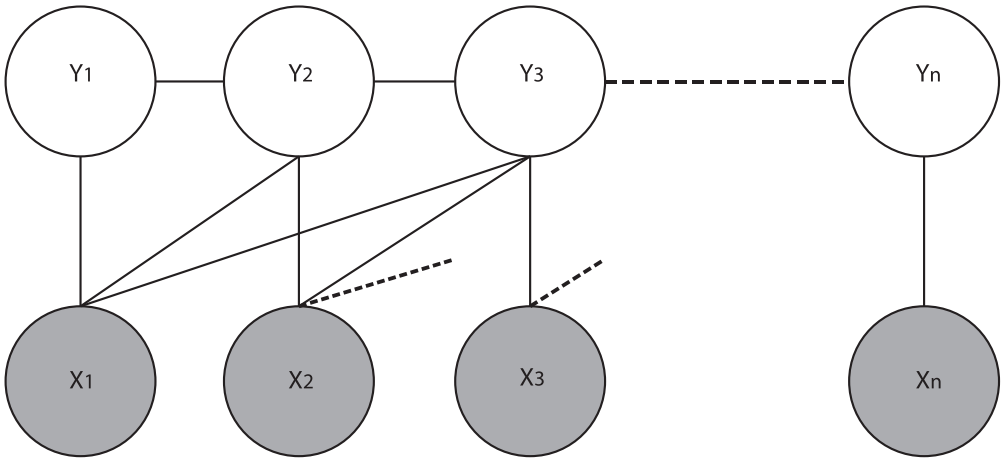

Figure 2. The CRF Model with long range dependencies. The label y_i at any time point i has a direct dependency on the current and two previous sample points of the brain signal features (0, 50 and 100 ms previous to the current time point.)

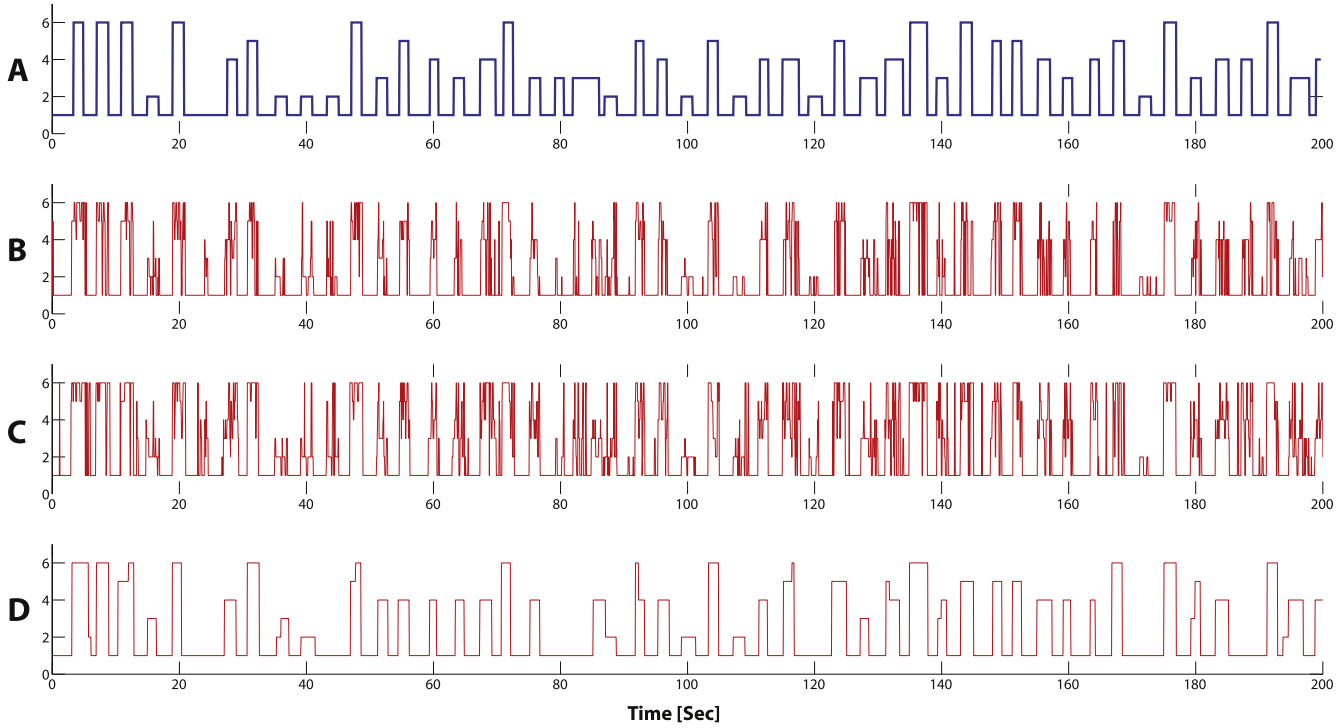

Figure 3. Comparison of the method's ouput classification for the same segment of brain signals. (Acc, Kappa, (σ (*Kappa*))) A. True Labels, B. Logistic Regression (Acc = 0.69, Kappa = 0.49(0.016)), C. Simultaneous Sparse Approximation (Acc = 0.67%, Kappa = 0.50(0.016)), D. Proposed method. (Acc = 0.71, Kappa = 0.54(0.017)).

weights, one for each class and each value of k. Therefore, the term $\sum_{l=0}^{k-1} \theta^T_{v_{(k,j)}} f_{v_j}(x_{(i-k,j)}, y_i)$ is a measure of the compatibility between the brain signals $x_{i-k:i}$ and the movement of the finger represented by the label y_i.

The edge potential function is defined as:

$$\Phi_i(y_i, y_{i-1}) = e^{\theta_e^T f_e(y_i, y_{i-1})} \tag{4}$$

where $f_e(y_i, y_{i-1}) = 1_{y_i, y_{i-1}}$. The term $1_{y_i, y_{i-1}}$ is a column vector of length 36 (the number of all the possible transitions between classes), with a non-zero entry at the position that represents the transition (y_i, y_{i-1}). The parameter θ_e is a set of weights of the same length as $1_{y_i, y_{i-1}}$. Therefore, the product $\theta_e^T f_e(y_i, y_{i-1})$ is a measure of the compatibility between the current state and the previous state, i.e., it provides a prior on the transition probabilities between classes. This information is useful given that it is known that the subject does not execute rapid changes between movement and rest. In this way, information about the dynamics of the task executed by the subject is incorporated in the model.

We learn the model parameters using training data by maximizing the following objective function

$$L(\theta) = \sum_i \log P(y_i|\mathbf{x}_i, \theta) - \lambda \frac{1}{2\sigma^2} \|\theta\|^2, \tag{5}$$

Figure 4. Classification results in terms of accuracy (confusion matrices) for each method across all subjects. Diagonals display the correct classification rate for each class.

Table 1. Overall accuracy for each subject.

Method	Subject 1	Subject 2	Subject 3	Average
LR	0.53	0.68	0.59	0.60
SSA	0.52	0.64	0.57	0.58
CRF	**0.62**	**0.69**	**0.65**	**0.65**

Table 2. Overall Coen's Kappa for each subject. (Standard error)

Method	Subject 1	Subject 2	Subject 3	Average
LR	0.40 (0.0078)	0.45 (0.0095)	0.46 (0.0084)	0.43
SSA	0.41 (0.0077)	0.45 (0.0090)	0.45 (0.0082)	0.43
CRF	**0.53** (0.0085)	**0.49** (0.0095)	**0.54** (0.0089)	**0.52**

where the first term in (5) is the log-likelihood of the data. The second term corresponds to a regularization term which is the log of a Gaussian prior with variance σ^2 and it is used to avoid over-fitting. The parameter λ is a regularization factor that determines how much penalty is imposed in the magnitude of the parameters θ. We used a quasi-Newton optimization algorithm using Hessian updates based on the Broyden–Fletcher–Goldfarb–Shanno (BFGS) formula to search for the optimal parameter values $\theta^* = \arg\max_\theta L(\theta)$. Given a new test sample $\mathbf{x}$ and parameter values θ^* induced from the training set, the label for a test sample is selected according to:

$$\bar{y} = \arg\max_{\mathbf{y}} P(\mathbf{y}|\boldsymbol{x}, \Theta) \tag{6}$$

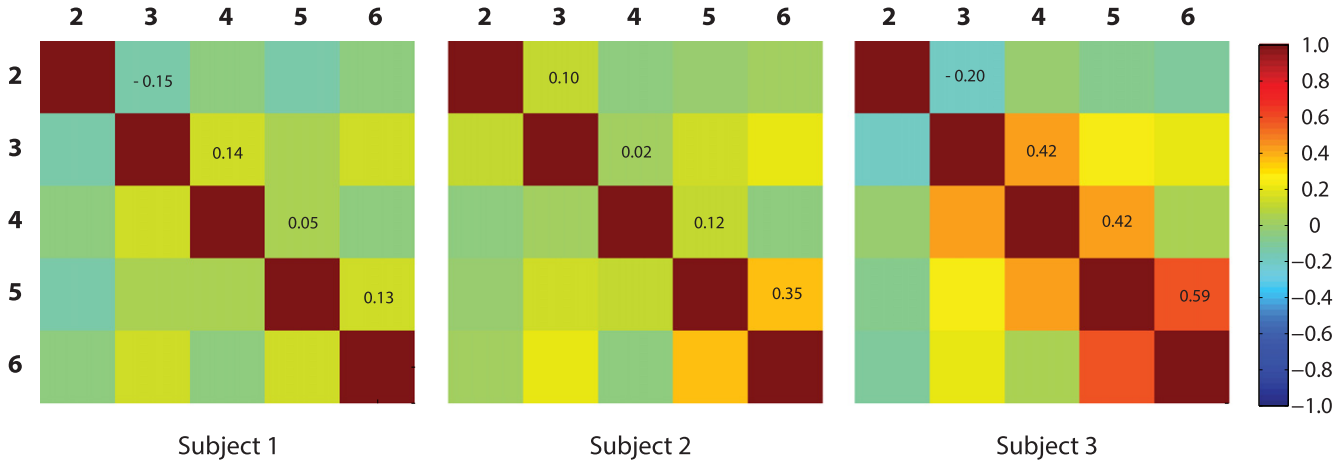

Figure 5. Estimated correlation matrix for the data-glove signals. Classes with labels 2-6 correspond to the movement of the fingers. Signals for rest are not included. For clarity, numerical values above the main diagonal, representing the correlations between adjacent fingers are shown.

4. Results

The whole data for each subject was divided into three sequential segments. A 3-fold cross-validation procedure was implemented, using each time two segments for training and the remaining segment for testing. The training set was further divided in two new sets in order to find the best value for the regularization factor λ. We compared our method against a baseline approach: logistic regression (LR). LR makes use of linear combination of the brain features to decide which finger is moving and it has this in common with the methods found in the literature. We also compared the proposed method to the Simultaneous Sparse Approximation (SSA) method proposed in [13] for detection of finger movements (see [25] for details on SSA). As discussed before, in the CRF model, long range dependencies can be used to account for the delay between the time that the brain signal is produced and the time that the fingers are moved. In the methods used for comparison (LR and SSA) this cannot be done directly. To address this limitation, and to make a fair comparison, we augmented the feature vector for LR and SSA in a way that it contains the actual signals and a delayed version of them with lags of 50 ms and 100 ms, which is equivalent to the use of long range dependencies in CRF.

The advantage of the CRF method is evidenced by the results displayed in figure 3. The proposed method takes into account the dynamics of the task and does not allow fast transitions in the predicted output. Contrary to this, LR and SSA methods produce an unstable output while detecting which finger is in motion. Further insight can be obtained by observing the classification results in terms of accuracy. To this end, for each time point the output of the classifier is compared with the ground truth and the percentage of correct number of classifications is reported. In order to have a better understanding of the performance of the classifiers, we present the confusion matrices averaged across subjects and cross-validation folds for each method in figure 4. The diagonal of each matrix shows the classification accuracy obtained for each class. Table 1 summarizes the results obtained for each subject in terms of classification accuracy. However, given that the number of samples for each class is not balanced in the data-set, we included the Coen's Kappa coefficient. Given that the subject passes from movement to rest before starting another movement, class 1 (rest) contains much more samples than the other classes. Therefore, accuracy above the chance level (17% for a six class classification problem) can be obtained by assigning all the outputs to class 1. Under these circumstances the classification accuracy could provide an unrealistic measure of the performance of the system. The Coen's Kappa coefficient does not present the sames issues described above for the classification accuracy, because it takes into consideration the empirical distribution of each class, which can be calculated using information from the confusion matrix [26] according to:

$$kappa = \frac{p_0 - p_e}{1 - p_e}, \tag{7}$$

where p_0 is the accuracy and p_e is the chance agreement given by:

$$p_e = \frac{\sum_{i+1}^{M} n_{:i} n_{i:}}{N^2} \tag{8}$$

where $n_{:i}$ and $n_{i:}$ are the sum of the ith column and the sum of the ith row of the confusion matrix, respectively. M is the number of classes and N is the total number of samples to test. Note that for a classification problem in which the number of samples for each class is equal, the parameter p_e is equal to $\frac{1}{M}$. The standard error for kappa is obtained by:

$$\sigma(kappa) = \frac{\sqrt{(p_0 + {p_e}^2 - \sum_{1}^{M}(n_{:i} + n_{i:})/N^3)}}{(1 - p_e)\sqrt{(N)}} \tag{9}$$

The standard error can be used to determine if the difference between two kappa values is statistically significant. Table 2 shows the kappa values obtained for each subject and the corresponding standard error. Using the standard error values we determined the statistical significance for the comparison between the proposed method and each one of the methods used for comparison. Statistically significant differences exist if the difference between the kappa values for two different methods is larger than two times the standard error. The results indicate that the improvement of the proposed method, over the methods used for comparison, is statistically significant as can be observed in table 2.

It is worth noting that logistic regression and conditional random fields belong to a general type of model known as a Log-linear model and the difference observed in the performance is entirely due to the incorporation of the information about the dynamics of the executed tasks. The proposed graphical model learns from the data (from the labels) that there are no rapid changes between the executed movements of the fingers. This information is captured by the model thanks to the incorporation of edge potentials (see equation (4)). These edge potentials measure the compatibility between the execution of a task in a particular time instant with the task executed in the previous time point.

From the confusion matrices in figure 4 we can observe that logistic regression only provides a better accuracy for the detection of the rest periods (periods of time in which the subject does not move any finger). However, this seems to be produced by a bias of the logistic regression towards this particular class. This bias is evidenced by results on the first row of the confusion matrix. These values indicate that the classifier, in many cases, confuses the movements of the fingers with rest periods. This can be explained by the fact that the number of samples in the training data for the rest periods are greater than the number of samples for any of the other classes. This issue is less critical in the proposed method while the SSA approach makes most of the mistakes confusing the movements of adjacent fingers.

Figure 4 shows that the highest misclassification rates are obtained between adjacent fingers. This could imply that when the subject is moving one finger, he or she also moves

the adjacent fingers. In order to verify this, we calculated the matrix of correlation values among the data-glove signals, which is displayed in figure 5. The correlation values found between adjacent fingers are statistically different from zero ($p < 0.01$). Also, the patterns observed in figures 4 and 5 are similar, which might support the idea that the subject may be moving more than one finger at the time, and that this might as well be the cause for the missclassification rate patterns found in figure 4. However, the correlation values observed could also be explained by the fact that there is a mechanical coupling among the sensors in the data-glove. Furthermore, the musculoskeletal structure of the hand will produce such an effect as well. Finally, neither the mechanical coupling of the data-glove sensors nor the musculoskeletal structure of the hand would alter the brain signals, and it is the brain signals on which the classification is based. We conclude that the correlations found between adjacent fingers cannot explain the pattern observed in the classification rates of the confusion matrices in figure 4. We conjecture that similar activity patterns are produced in the brain during the movement of adjacent fingers and that this explains the observed patterns in the confusion matrices. We propose that the incorporation of spatial relationships between different brain regions, together with the temporal structure of the signals, should be modeled in order to improve the classification performance. We believe that this spatio-temporal structure could be efficiently modeled using probabilistic graphical models.

5. Conclusion

In this work, we propose a method based on conditional random fields to classify finger movements from ECoG signals. The proposed method makes use of information about the activity in high gamma (including long range dependencies) as well as information about the temporal dynamics of the task executed by the subject. The results show that the performance of the system is effectively increased by adding and modeling the extra piece of information related to the dynamics of the task. We suggest that this type of model holds the potential to incorporate temporal dynamics as well as spatial features (such as which areas of the brain are activated and how they interact). This could provide a model that better explains the brain signals generated during the execution of specific mental tasks.

Acknowledgments

This work was partially supported by Universidad del Norte (Colombia), the Scientific and Technological Research Council of Turkey under Grant 111E056, and by Sabanci University under Grant IACF-11-00889.

References

[1] Leuthardt E C, Schalk G, Wolpaw J R, Ojemann J G and Moran D W 2004 A brain computer interface using electrocorticographic signals in humans *J. Neural Eng.* **1** 63
[2] Schalk G and Leuthardt E 2011 Brain-computer interfaces using electrocorticographic signals *Biomedical Engineering IEEE Reviews in* **4** 140–54
[3] Brunner P, Ritaccio A L, Emrich J F, Bischof H and Schalk G 2011 Rapid communication with a 'p300' matrix speller using electrocorticographic signals (ecog) *Front Neurosci* **5** 5 02/2011
[4] Blakely T M, Olson J D, Miller K J, Rao R P and Ojemann J G 2014 Neural correlates of learning in an electrocorticographic motor-imagery brain-computer interface *Brain-Computer Interfaces* **1** 147–57
[5] Kapeller C, Kamada K, Ogawa H, Prueckl R, Scharinger J and Guger C 2014 An electrocorticographic bci using code-based vep for control in video applications: a single-subject study *Frontiers in Systems Neuroscience* **8** 139
[6] Eliseyev A *et al* 2014 Clinatec® bci platform based on the ecog-recording implant wimagine® and the innovative signal-processing: Preclinical results, in Engineering in Medicine and Biology Society (EMBC) *2014 36th Annual International Conference of the IEEE* pp 1222–5
[7] Vogel J, Haddadin S, Jarosiewicz B, Simeral J, Bacher D, Hochberg L, Donoghue J and Van Der Smagt P 2015 An assistive decision-and-control architecture for force-sensitive hand-arm systems driven by human-machine interfaces *Int. J. Robot. Res.* **34** 763–80
[8] Athanasiou A, Chatzitheodorou E, Kalogianni K, Lithari C, Moulos I and Bamidis P 2010 Comparing sensorimotor cortex activation during actual and imaginary movement *XII Mediterranean Conference on Medical and Biological Engineering and Computing 2010 IFMBE Proc.* vol 29 (ed P Bamidis and N Pallikarakis (Berlin: Springer) pp 111–4
[9] Kubánek J, Miller J W, Ojemann J G, Wolpaw J R and Schalk G 2009 Decoding flexion of individual fingers using electrocorticographic signals in humans *J Neural Eng.* **6** 066001
[10] Wang Z, ji q, Miller K J and Schalk G 2011 Prior knowledge improves decoding of finger flexion from electrocorticographic (ecog) signals *Frontiers in Neuroscience* **5** 127
[11] Wissel T, Pfeiffer T, Frysch R, Knight R T, Chang E F, Hinrichs H, Rieger J W and Rose G 2013 Hidden markov model and support vector machine based decoding of finger movements using electrocorticography *J. Neural Eng.* **10** 056020
[12] Liao K, Xiao R, Gonzalez J and Ding L 2014 Decoding individual finger movements from one hand using human eeg signals *PLoS ONE* **9** e85192 01
[13] Flamary R and Rakotomamonjy A 2012 Decoding finger movements from ECoG signals using switching linear models *Frontiers in Neuroscience* **6** 29
[14] Miller K J, Honey C J, Hermes D, Rao R P, denNijs M and Ojemann J G 2014 Broadband changes in the cortical surface potential track activation of functionally diverse neuronal populations Part 2, New Horizons for Neural Oscillations. *NeuroImage* **85** 711–20
[15] Wang W *et al* 2009 Human motor cortical activity recorded with Micro-ECoG electrodes, during individual finger movements *Engineering in Medicine and Biology Society, 2009. EMBC 2009. Annual International Conference of the IEEE* pp 586–9
[16] Delgado Saa J and Cetin M 2011 Hidden conditional random fields for classification of imaginary motor tasks from eeg

data *European Signal Processing Conference, EUSIPCO* pp 171–5
[17] Saa J F D and Çetin M 2012 A latent discriminative model-based approach for classification of imaginary motor tasks from eeg data *Journal of Neural Engineering* **9** 026020
[18] Delgado Saa J and Cetin M 2013 Discriminative methods for classification of asynchronous imaginary motor tasks from eeg data *Neural Systems and Rehabilitation Engineering, IEEE Transactions on* **21** 716–24
[19] Saa J F D, de Pesters A, McFarland D and etin M 2015 Word-level language modeling for p300 spellers based on discriminative graphical models *J. Neural Eng.* **12** 026007
[20] Martens S, Farquhar J, Hill J and Scholkopf B 2009 Graphical models for decoding in bci visual speller systems *Neural Engineering, 2009. NER '09 4th International IEEE/EMBS Conference* pp 470–3
[21] Obermaier B, Guger C, Neuper C and Pfurtscheller G 2001 Hidden markov models for online classification of single trial eeg data *Pattern Recognition Letters* **22** 1299–309
[22] Schalk G, Kubnek J, Miller K J, Anderson N R, Leuthardt E C, Ojemann J G, Limbrick D, Moran D, Gerhardt L A and Wolpaw J R 2007 Decoding two-dimensional movement trajectories using electrocorticographic signals in humans *J. Neural Eng.* **4** 264
[23] Ray S, Crone N E, Niebur E, Franaszczuk P J and Hsiao S S 2008 Neural correlates of high-gamma oscillations (60-200 hz) in macaque local field potentials and their potential implications in electrocorticography *J. Neuroscience* **28** 11526–36
[24] Wang Z, Ji Q, Miller J W and Schalk G 2011 Prior knowledge improves decoding of finger flexion from electrocorticographic signals *Frontiers in Neuroscience* **5** 127 11/2011
[25] Rakotomamonjy A 2009 Algorithms for multiple basis pursuit denoising *in SPARS'09-Signal Processing with Adaptive Sparse Structured Representations* https://hal.inria.fr/inria-00369535/
[26] Dornhege G 2007 *Toward Brain-Computer Interfacing* (Cambridge, MA: MIT Press)